

ANALYSIS OF A COMBINED RADIAL-AXIAL MAGNETIC BEARING FOR A HIGH-SPEED DRIVE SYSTEM

Philipp Imoberdorf*, Thomas Nussbaumer[†], Johann W. Kolar*

*Power Electronic Systems Laboratory, ETH Zurich, 8092 Zurich, Switzerland, imoberdorf@lem.ee.ethz.ch

[†]Levitronix GmbH, Technoparkstrasse 1, 8005 Zurich, Switzerland

Keywords: magnetic bearing, coupling effects, permanent magnet machine

Abstract

High-speed and high-power-density drives are attracting much interest in today's industry, e.g. for applications with mesoscale gas turbine generator systems or turbocompressors for fuel cells. In all high-speed machinery the bearing is a key component. Therefore, this paper presents the analysis of an active magnetic bearing suitable for a permanent magnet machine, being part of a high-speed electrical drive system. The focus is on the detailed analysis of the magnetic forces, the coupling between the different axes and the verification of the theoretical considerations by means of 3D-FEM simulations. The analysis of the bearing forces is needed to implement the position control to the prototype of the bearing system, which already has been built.

1 Introduction

Over the last few years, industry has had an increasing need for high-speed and high-power-density drives, and the trend to more compact and higher speed drives continues [1]. For instance, in the PCB drilling industry the trend is to produce smaller diameter holes and in order to attain the same productivity as today the drilling machines have to rotate at much higher speeds (more than 300,000 rpm). The trend for turbocompressors is towards smaller power ratings and with the scaling of turbo machinery, they therefore require higher operating speeds [2], [3]. One application is in a fuel cell air compressor that requires 120,000 rpm at 12 kW [4] and another is in a 70,000 rpm, 131 kW turbo compressor connected to a PM machine and inverter [5]. Future automotive fuel cells will require low power air compressors, which are small and lightweight, and directly driven by high-speed electrical drives. Ultra-micro gas turbines with power outputs up to several hundred watts are being investigated for use in portable power applications [6].

A key technology for all high-speed rotating machinery is the bearing system. Therefore, this paper presents the design and analysis of an active magnetic bearing suitable for a permanent magnet machine, which is part of a high-speed electrical drive system. The machine and the magnetic bearings are integrated into one system and the power and control electronics for both drive and bearing are optimised for high-speed operation and minimal volume. The

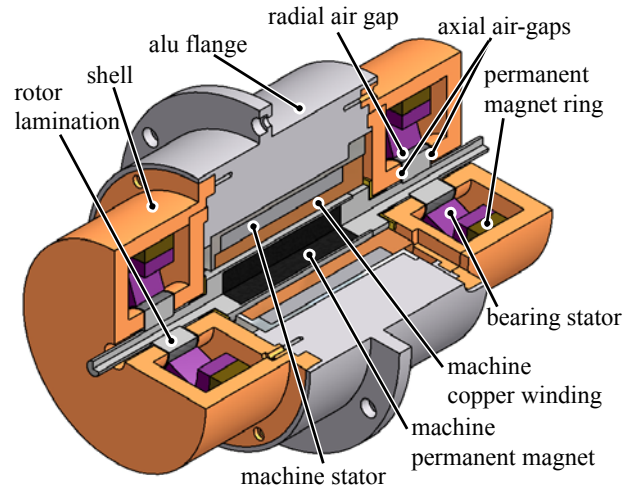


Fig. 1. Cut-away view of the electrical drive and the two radial-axial bearing units mounted on two sides.

motivation for this work is to achieve a compact design of a combined radial-axial magnetic bearing to ensure a compact drive system.

In section 2, the design of the magnetic bearing and mechanical construction is presented. The behaviour of the bearing forces in the combined radial-axial magnetic bearing is further described in section 3. Furthermore the bearing behaviour derived from simplified analytical calculations is compared with 3D-FEM results. The implications of the presented characteristics of the bearing forces on the control of the magnetic bearing are presented in section 5. Finally, a summary is given and the future work for the combined radial-axial magnetic bearing is discussed.

2 Concept / System

The active magnetic bearing is constructed together with a 1 kW, 500'000 rpm permanent-magnet machine developed at ETH Zurich [1]. The machine and the magnetic bearings are integrated into one system and the power and control electronics for both the drive and bearing are optimised for high-speed operation and minimal volume. The rotor is driven by a 1 kW permanent magnet synchronous machine and a bearing unit is placed at each end of the rotor as depicted in Fig. 1. The overall size of the system is a maximum diameter of 55 mm and a rotor length of 96 mm.

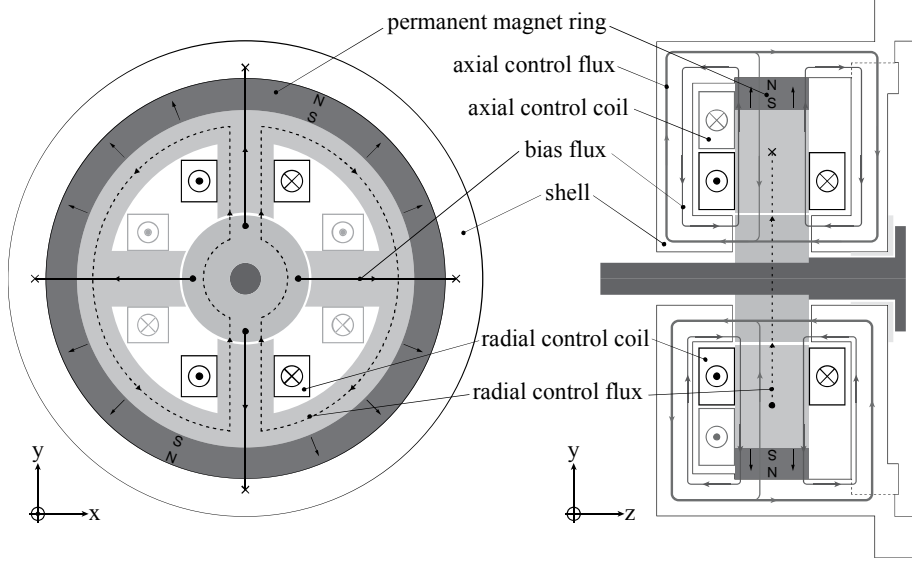


Fig. 2. Axial and radial cut view showing the magnetic flux paths.

Most of the active magnetic bearing systems have two separate bearings for the axial and the radial direction. This is the easiest way to produce a magnetic bearing but it also requires more space for the two separate devices. In order to reduce the overall size of the bearing and drive system, which is an important consideration in ultra-compact high-speed machines, the combination of the radial and axial bearing is one attractive possibility. The chosen concept, depicted in Fig. 2, combines the two bearings by using a radially magnetised permanent magnet ring as source of the bias flux for both the radial and the axial bearing [7]. The bias flux created by the permanent magnet ring alone does not provide any force. It has to be superimposed by a control flux for both the radial and the axial bearing force. In Fig. 2, both the radial and the axial control flux paths are depicted. In one air gap, the bias flux and the control flux add together, whereas in the opposing air gap they subtract. The resulting difference of magnetic flux density in these two air gaps creates the carrying force and can be controlled by the sign and amplitude of the control current in the control coils. The bearing force in one air-gap is deduced from the stored magnetic energy in the air-gap. Applying this to the case, where there are two opposite forces and the magnetic field is created by a bias flux density B_0 combined with a control flux density B_c results in a total magnetic force acting on the rotor according to

$$F = \frac{2A_\delta}{\mu_0} \cdot B_0 B_c, \quad (1)$$

where A_δ is the active pole shoe area. For small deflections x of the shaft position the bearing force F_x in x -direction can be linearised for very simple cases as

$$F_x = k_{ix} \cdot i_x + k_{rx} \cdot x, \quad (2)$$

where k_{ix} is the force-current factor and k_{rx} the force-displacement factor in x -direction. k_r is also called negative stiffness of the magnetic bearing since without a

control current the force acts as a negative spring force and thus is instable. The idea is to characterise the magnetic bearing via these two parameters. For the shown concept it will be shown that the relation is not that simple. The force is not only linearly dependent on the position and the current. Thus the force in the x -direction is better described by

$$F_x = f(i_x, x). \quad (3)$$

The technical challenge of the shown concept consists in the fact that during operation the force F_x is not only dependent on i_x and x but is depending on the actual position of the rotor in all directions (x, y, z) as well as on the control currents i_x, i_y and i_z in the different coils. This leads then to the following characterisation of the bearing force F_x

$$F_x = f(i_x, i_y, i_z, x, y, z). \quad (4)$$

For all three forces $\mathbf{F} = (F_x, F_y, F_z)^T$ this relation can be rewritten as

$$\mathbf{F} = f(\mathbf{i}, \mathbf{r}), \quad (5)$$

where $\mathbf{r} = (x, y, z)^T$ is the vector defining the actual position of the rotor and $\mathbf{i} = (i_x, i_y, i_z)^T$ is the vector containing the values of the actual control currents for each direction.

3 Analysis of the Bearing Forces

In order to characterise the bearing by the expanded equation (5) and to analyze the system stability for different points of operation a model of the combined radial-axial magnetic bearing has to be built. In a first approach, the magnetic bearing is modelled as an equivalent magnetic circuit as depicted in Fig. 3. Hereby, the permanent magnet is modelled by a magnetic voltage source θ_{PM} in series with the reluctance R_{PM} . The reluctances of the airgaps are dependent on the dimensions of the airgap and are defined as

$$R_\delta = \frac{l_\delta}{\mu_0 A_\delta}, \quad (6)$$

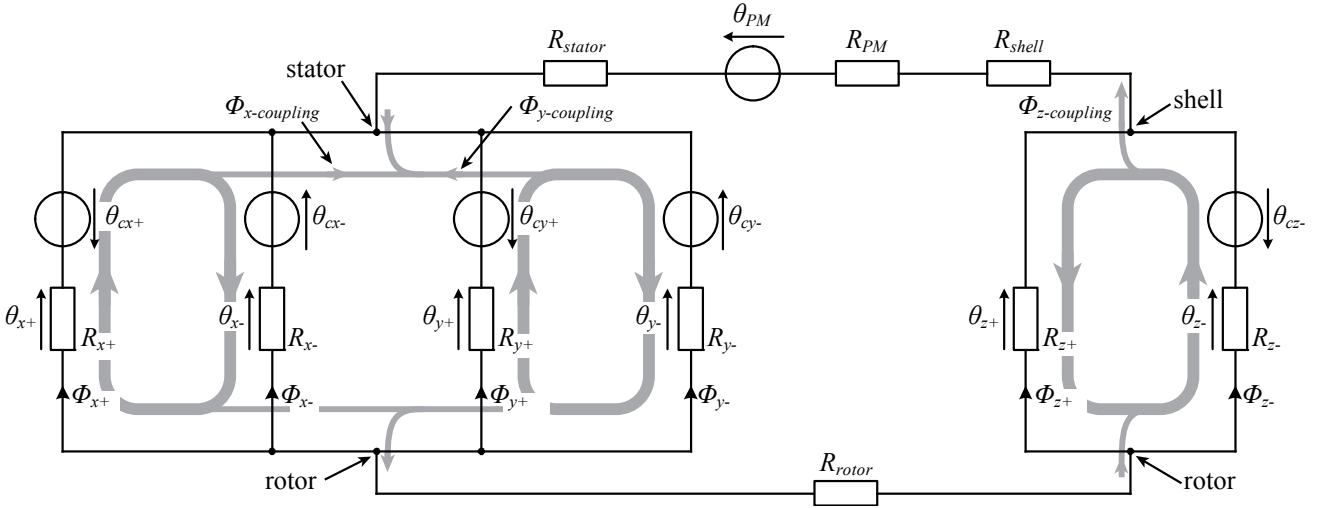


Fig. 3. Equivalent magnetic circuit for the magnet fluxes of the combined radial-axial bearing.

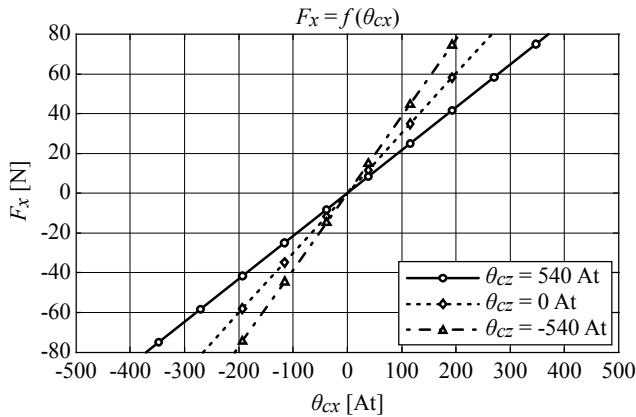
for a homogenous field distribution within the gap. In reality, also stray flux effects have to be considered by adjusting the effective airgap length and its effective cross section. This can be done by comparative 3D-FEM simulations as performed in section 4. The currents injected in the control coils are modelled as magnetic voltage sources θ_{cx+} , θ_{cx-} , θ_{cy+} , θ_{cy-} and θ_{cz-} . As the control coils for each radial bearing are connected in series, the two corresponding voltage sources are oriented such that their magnetic fluxes add together in the main magnetic path. In Fig. 3 the main magnetic paths for the three bearing directions are illustrated by the bold gray lines. The hereby created control flux originates in the negative stator-tooth, passes through the rotor and enters the positive stator-tooth. Looking at Fig. 2 this can be verified for the y-axis. Due to the equal ampere-turns in each axis, the condition

$$\theta_{cx+} = \theta_{cx-} = \theta_{cx} \text{ and } \theta_{cy+} = \theta_{cy-} = \theta_{cy} \quad (7)$$

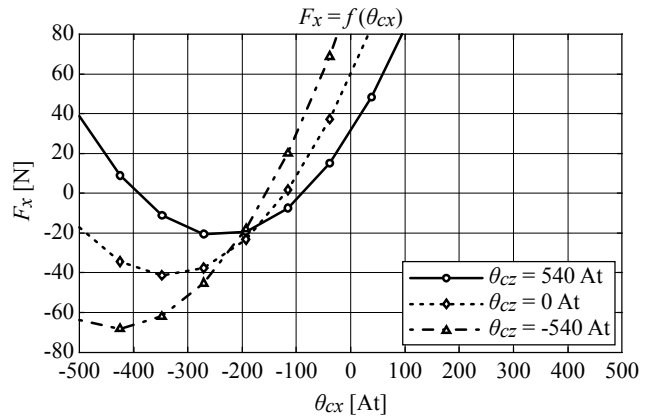
is true. Assuming the rotor in its centre position, the radial airgap reluctances R_{x+} , R_{x-} , R_{y+} and R_{y-} are equal. Therefore, the magnetic flux created by θ_{cx+} and θ_{cx-} will flow entirely in the main magnetic path depicted in bold gray on the left side

of Fig. 3. However, if we assume the rotor to be displaced in x-direction, the reluctances R_{x+} and R_{x-} differ and therefore not the entire flux will flow in the main path. Part of it will flow through the airgaps in the y-axis and the z-axis and consequently constitute a coupling flux $\Phi_{x-coupling}$. Thus, if all the radial reluctances are equal – the rotor is then in its centre position – the y-axis is independent of the control flux created by the magnetomotive force θ_{cx} . On the other hand if the rotor is deflected from its centre position the four radial airgap reluctances are not equal anymore. Due to such an asymmetry the magnetomotive force θ_{cx} can also create a force in the y-direction. The same reasoning can be done for the flux created by θ_{cz} . Since the permanent magnet ring has a big cross section, its reluctance is of comparable dimension as the airgap reluctances and therefore the permanent magnet reluctance is not a perfect separation of the axial and the radial magnetic flux paths. Therefore, part of the flux created by θ_{cz} will flow as a coupling flux $\Phi_{z-coupling}$ through the radial airgaps.

In Fig. 4 the dependency of the radial force F_x on different parameters is shown for small airgaps of $250 \mu\text{m}$. For

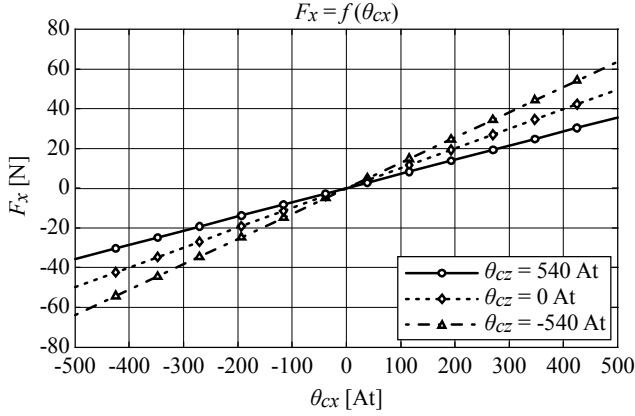


(a)

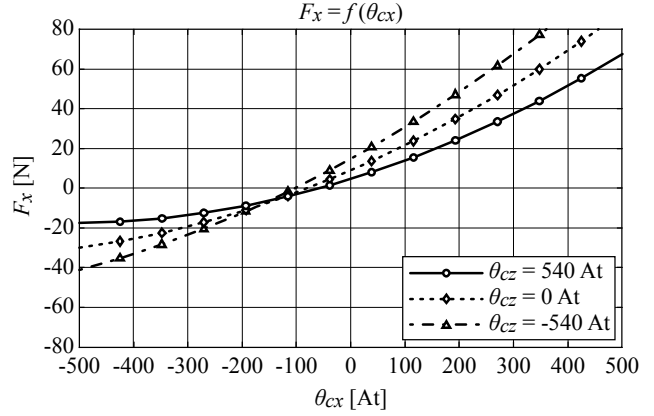


(b)

Fig. 4. Calculation of the radial force-current relation for (a) $x = 0 \mu\text{m}$ and (b) $x = 150 \mu\text{m}$ for a nominal airgap of $\delta = 250 \mu\text{m}$.



(a)



(b)

Fig. 5. Calculation of the radial force-current relation for (a) $x = 0 \mu\text{m}$ and (b) $x = 150 \mu\text{m}$ for a nominal airgap of $\delta = 500 \mu\text{m}$.

Fig. 4(a) the rotor is assumed to be in its centre position. With the magnetomotive force θ_{cx} varying and θ_{cy} set to zero ampereturns, three curves for the force F_x for three different magnetomotive forces θ_{cz} are depicted. One can see that θ_{cz} from the axial axis has an influence on the radial force but still the relation between the current i_x and the force F_x is linear for all cases. The influence of θ_{cz} gets obvious as we look at the coupling flux $\Phi_{z\text{-coupling}}$. This flux increases the main flux created by θ_{cx} in the negative airgap x_- , but decreases the main flux in the positive airgap x_+ . So the force-current relation in the x -axis is weakened for positive z -currents as shown in Fig. 4(a). The situation changes when an additional radial displacement $x = 150 \mu\text{m}$ occurs. The relation between the force F_x and the magnetomotive force θ_{cx} becomes highly non-linear. Such a non-linear characteristic and the coupling to the other axes' parameters can pose severe problems for the control of the rotor position as will be shown in the next section.

We can now compare these results with a bearing with increased airgaps of $\delta = 500 \mu\text{m}$. This will result in lower bearing forces for the same amount of magnetomotive force but can improve the non-linear relation of the control current and the created force. In Fig. 5(a) it can be seen that the force F_x is substantially lower than it is in the bearing system with tight airgaps. On the other hand, when the rotor is deflected in x -direction, the nonlinearity is much less pronounced in Fig. 5(b) than it is in Fig. 4(b) for the small airgaps. In fact, the nonlinear behaviour gets more dominant the smaller the margin between rotor and stator is. Therefore, for rotor movements of $\pm 150 \mu\text{m}$ it may be better to choose an airgap that is at least $500 \mu\text{m}$.

The two charts show that in all situations there is an ampere-turns value θ_{cx} , for which the rotor can be pulled to and held in the centre position. In such a stationary analysis the rotor can be stabilised by a correct choice of the control current. However, it is important to keep in mind that with a too narrow airgap the stabilisation can be much more difficult to achieve since the controller has to guarantee a stable operation even under non-linear conditions. This is not trivial since a magnetic bearing on its own is already challenging in

terms of stable control due to the inherent unstable characteristics of the control path. A proper selection of the PID controller gains is a basic requirement for a stable operation. If the control path changes such strongly as described in Fig. 4 and Fig. 5 due to different operating points of the bearing, it will be a big challenge for a stable control within the whole range of operation.

4 Verification with 3D-FEM

As the nonlinear relations between the magnetic forces and the operating point parameters are used in the control for the bearing, the validity of the simplified analytical model has to be verified. This has been done by modelling the magnetic bearing in a 3D-FEM simulation software [8]. In all the simulations both the radial and the axial airgaps are set to $500 \mu\text{m}$. The results of the simulations showed that the magnetic flux is not entirely confined in the airgap area but also takes some stray paths. This fact has to be considered in the analytical model of the equivalent magnetic circuit. This was done by adjusting the airgap reluctances for the increased airgap area as mentioned before.

For the comparison in Fig. 6 the relation of the axial force and the axial control flux was studied. In the simulation the stator material is defined as a real magnetic iron. Therefore,

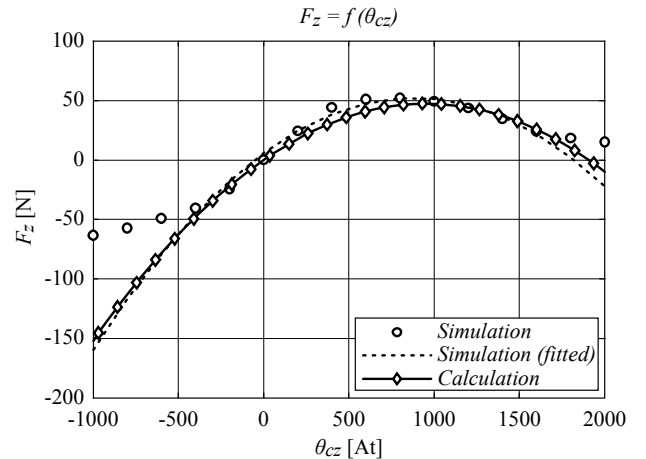


Fig. 6. Comparison of the axial force-current relation derived by calculation and by a 3D-FEM simulation.

saturation effects occur for high magnitudes of current injection into the control coils. The outermost dots on each side in Fig. 6 were ignored for the fitted curve of the simulation results because saturation effects in the range of high control fluxes are not considered in the analytical model. As can be seen in the chart, the force calculated with the equivalent magnetic circuit coincides well with the results from the 3D-FEM simulation, which confirms the proposed model.

In Fig. 7 the effect of a deflected rotor on the radial force is depicted. In one case the rotor is in its centre position and no other current than i_x is present. The second pair of curves shows the situation when the rotor is deflected in the positive x -direction by $200 \mu\text{m}$. Again, an acceptable match of the simulation and calculation results can be observed. This proves the presented analytical model which therefore can be used for the controller design.

5 Effects on the Control

The main challenge in a magnetic bearing is always a stable and robust levitation of the rotor either in its centre position or in another predefined position. The control of the rotor position will be implemented as cascaded position controller. To study the effects of the non-linear relations in the magnetic bearing system the cascaded controller was implemented as a Matlab/Simulink model. The performance of the controller can be compared for different definitions of the forces. A first approach is to define the force according the well-known relation (2) where k_i and k_r are taken from the simplest operating point where the rotor is in its centre position and no control currents are injected into the coils. In this first simulation of the cascaded position controller the force-current and the force-displacement factors were defined as follows:

	Radial bearing	Axial bearing
Force-current factor - k_i	2.8 [N/A]	6.1 [N/A]
Force-displacement factor - k_r	64 [N/mm]	172 [N/mm]

Table 1. Bearing parameters describing the carrying force for a linearised model.

Thus, the force in each direction is assumed to be linearly dependent only on the control current in the corresponding coil and on the deflection of the rotor in that axis. The bearing parameters k_i and k_r are assumed to remain constant for any position the rotor can reach and for any current injected in the coils. For such a model it is possible to find a PID parameter set which stabilises the rotor or to let it follow a certain setpoint function.

It should now be investigated if the aforementioned non-linear characteristics of the bearing forces pose a problem for such a controller. To simplify the problem only the definition of the force for the x -axis is made variable. All the other bearing parameters are left unchanged. As it can be observed in Fig. 8 the force F_x no longer depends linearly on the control magnetomotive force θ_{cx} if the rotor is deflected in x -direction. Knowing that the magnetomotive force θ_{cx} is

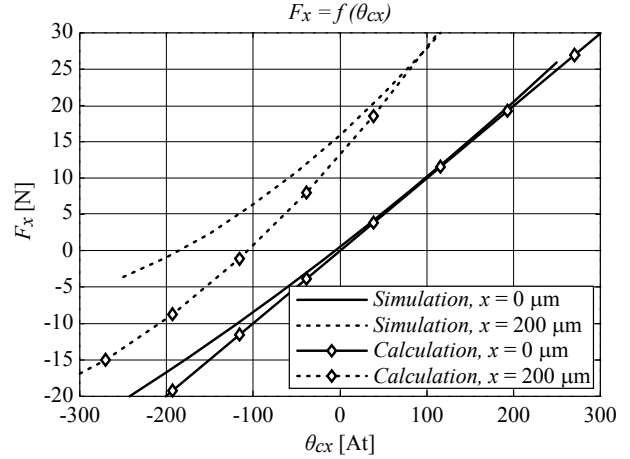


Fig. 7. Comparison of the radial force-current relation for two different radial positions derived by calculation and by a 3D-FEM simulation.

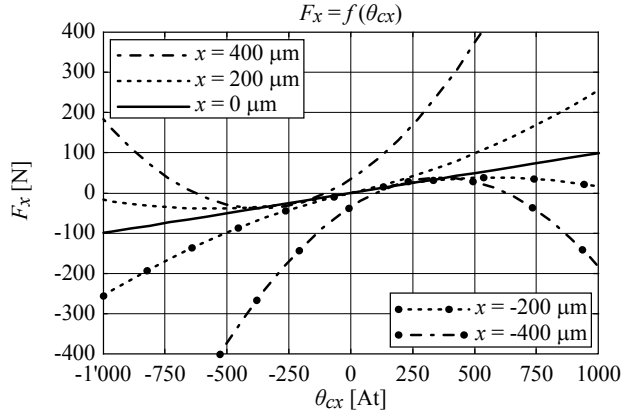


Fig. 8. Nonlinear dependency of F_x on displacement x .

directly related to the control current i_x via the number of turns, the relation of the force F_x and the control current can now be described by a function according to the following polynomial equation:

$$F_x = a(x) \cdot i_x^2 + b(x) \cdot i_x + c(x), \quad (8)$$

where the polynomial coefficients are dependent on the rotor displacement in the x -direction. The coefficients for the curves depicted in Fig. 8 are listed in Table 2. These coefficients were then integrated in the simulation model of the controller. In reality however, the polynomial coefficients are also dependent on the rotor deflection in the other directions and also depend on the control currents in the other coils. This fact has been omitted in order to simplify the problem.

In Fig. 9 the rotor position should follow a sinusoidal setpoint function. If we implement the constant bearing parameters

displacement x	a	b	c
centre position	0	2.7872	0
$\pm 200 \mu\text{m}$	± 0.0934	3.8110	± 13.077
$\pm 400 \mu\text{m}$	± 0.4308	11.2304	± 60.302

Table 2. Bearing parameters describing the carrying force.

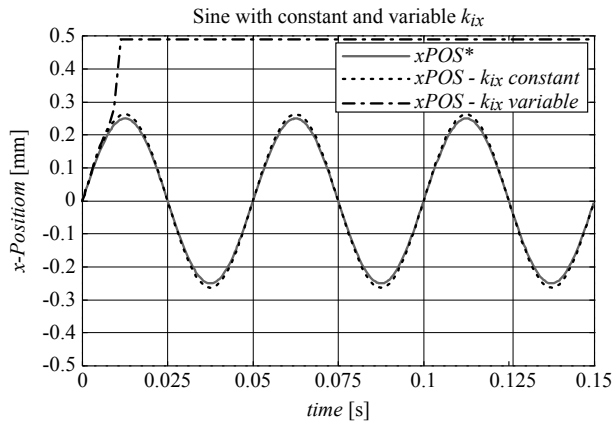


Fig. 9. Controlled x -position following a sinusoidal set-point.

listed in Table 1 there can be found a PID parameter set (K_P , T_I , T_D) which makes the rotor follow the setpoint function. Now it should be checked if the controller works as well if the force F_x is dependent on the rotor position as described in equation (8) with the parameters of Table 2. As can be seen in Fig. 9 this is not the case for the same set of PID parameters. The x -position of the rotor cannot follow the sinusoidal setpoint function and the rotor can't be pulled to the centre anymore with this set of PID parameters. A similar behaviour can be observed if we force the rotor to follow a stepfunction as depicted in Fig. 10.

Thus, it is essential to implement the correct definitions for the different forces with their dependencies on the current operating point of the magnetic bearing in order to optimise the position controller. It may be necessary to implement a non-linear controller or a decoupling network to linearise the control path. Or it may be even possible that the bearing parameters have to be adapted during operation according the actual working point.

6 Summary

For high-speed machines the use of conventional ball bearings brings some drawbacks as high losses and limited lifetime. An active magnetic bearing is an alternative bearing topology, which is suitable for high-speed operation. Due to the compact size of the electrical machine at these high-speeds, it is important to minimise the volume of the magnetic bearing as well. In this paper, an active magnetic bearing that has the radial and axial forces combined into a single bearing unit was presented.

One of the critical and challenging research topics for active magnetic bearings is the analysis of the magnetic forces, their dependencies and their couplings. For this purpose, a simple analytical model of the bearing was described. With this model the bearing forces were discussed and some important dependencies and couplings were pointed out. To validate the analytical model it has been compared to the results of 3D-FEM simulations of the chosen bearing system. The simulation results showed a good accordance with the analytical results, which confirms the proposed model. Both approaches clearly showed the nonlinear characterisation of the bearing forces depending on the bearing's current

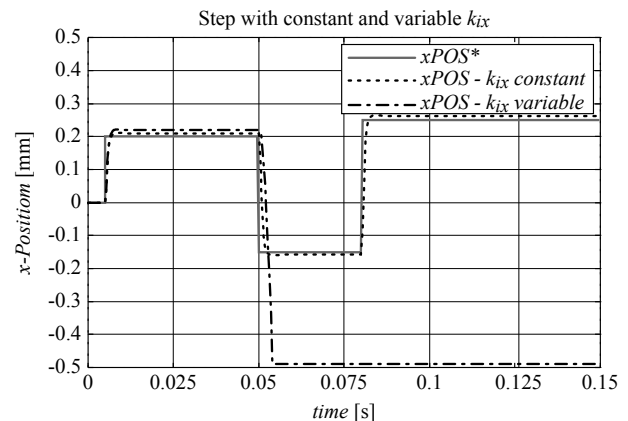


Fig. 10. Controlled x -position following a stepfunction as set-point.

operating point. Furthermore, the effects of this non-idealities on the position controller of the bearing were studied. It can be concluded that the correct description of the bearing forces is crucial in order to find the appropriate PID controller gains. It may be even necessary to adapt the controller gains during operation according the current operating point. Further research in that field will be focused on the analysis of small-signal and large-signal stability of the control for such a coupled system under consideration of decoupling networks. Furthermore, the cross-coupling between the bearing axes shall be minimised and geometrical parameters will be studied in order to achieve stable control behaviour.

References

- [1] C. Zwyssig, M. Dürr, S.D. Round and J.W. Kolar, "An Ultra-High-Speed, 500'000 rpm, 1 kW Electrical Drive System," 4th Power Conversion Conference 2007, Nagoya, Japan, April 2-5, 2007.
- [2] M. A. Rahman, A. Chiba, and T. Fukao, "Super high speed electrical machines – summary," IEEE Power Engineering Society General Meeting, June 6-10, 2004, vol. 2, pp. 1272 – 1275.
- [3] J. Oyama, T. Higuchi, T. Abe, K. Shigematsu, X. Yang, E. Matsuo, "A trial production of small size ultra-high speed drive system," IEMDC2003, vol. 1, no.2-1-1, pp. 31 – 36, 2003.
- [4] MiTi Developments (November 2005). "Oil-free, motorized, automotive fuel cell air compressor/expander system," Available: <http://www.miti.cc>
- [5] B. H. Bae, S. K. Sul, J. H. Kwon, and J. S. Byeon, "Implementation of sensorless vector control for super-highspeed PMSM of turbo-compressor," IEEE Trans. on Industry Applications, vol. 39, no. 3, pp. 811 – 818, May-Jun. 2003.
- [6] S. A. Jacobson and A. H. Epstein, "An informal survey of power MEMS," ISMME2003, Tsuchiura, Japan, December 1 – 3, 2003, pp. 513 – 520.
- [7] P.T. McMullen, S. Huynh, "Magnetic Bearing Providing Radial and Axial Load Support for a Shaft," U.S. Patent 5,514,924, May 7, 1996.
- [8] Maxwell 3D by Ansoft Corporation [Online]. Available: <http://www.ansoft.com>.